

# Modal Truncation, Ritz Vectors, and Derivatives of Closed-Loop Damping Ratios

Chris A. Sandridge\* and Raphael T. Haftka†

*Virginia Polytechnic Institute and State University, Blacksburg, Virginia 24061*

**The effect of modal truncation on the damping ratio and their derivatives with respect to an added mass is investigated for a simply supported, multispan beam with a linear quadratic Gaussian control system. It is found that both the damping ratios and derivatives converge slowly, but the derivatives converge more slowly than the damping ratios. However, it is shown that when Ritz vectors corresponding to static displacements due to actuator forces are added to the reduced model, the convergence of both the damping ratios and their derivatives is accelerated. It is also shown that the accuracy of the damping ratio predicted by a reduced-model control design can be improved significantly if the Ritz vectors are included in the design of the control system. Thus, it appears that Ritz vectors added to the reduced model of flexible structures can improve greatly the accuracy of both the design and analysis of the control system.**

## Introduction

As a result of the high cost of transporting mass into space, large space structures (LSS) are expected to be very flexible and have little inherent damping; thus, control systems will be needed to damp out vibrations. The control system can consist of passive damping, active control, or a combination of the two. The design process has typically proceeded in two steps. First, a structural engineer would design the structure to minimize the weight while meeting specified stress and geometric constraints. Then a control engineer would design passive damping treatments and an active control system to provide the necessary damping. Recently, however, there has been interest in combined structure-control system design (see, for example, Refs. 1-4). This is based on indications that small changes in the structure can reduce significantly the control effort needed to damp vibrations, thus lowering the total cost of the structure and control. Therefore, such combined structure-control designs typically require the derivatives of the closed-loop eigenvalues with respect to structural parameters.

One of the major problems in the design of control systems for LSS is how to model the structure accurately. The finite element model of a structure can have thousands of degrees of freedom, which makes it impractical for use in control system design; therefore, some type of reduced model must be used. In control system design, a reduced model based on a small number of vibration modes is typically used to model the structural dynamics. However, the errors associated with the reduced model can cause the control system to become unstable. For example, spillover instability is associated with the excitation of higher-order modes that are not included in the reduced model.<sup>5</sup> However, it is usually possible to overcome these instabilities by special techniques (e.g., Ref. 6) or by building enough robustness into the control design.

The reduced models used for control design are usually based on the lowest natural vibration modes according to frequency. This procedure may neglect important higher frequency modes, since for an LSS, the higher modes can still have very low frequencies and strong coupling with the lower modes. Modal cost analysis techniques were developed for choosing the best modes to include in the model.<sup>7-9</sup> Each mode is assigned a cost depending on characteristics of the mode, the type of control system, the type of analysis or design being performed, and the location of the sensors and actuators for the case of control design. The costs are then used to decide which vibration modes should be included in the reduced model.

To integrate the control and structural designs, the sensitivity of the control system to changes in the structure is needed. It has been shown that the convergence of the derivatives of the structural response with an increasing number of modes can be much slower than the convergence of the response itself.<sup>10</sup> That is, more modes are required to calculate the derivatives accurately. The problem of slow modal convergence of derivatives can be expected to be more severe for LSS that typically have a large number of closely spaced frequencies.

Modal expansion is a generalization of the Fourier series. It is well known that Fourier series of discontinuous functions converge slowly with respect to the number of series terms, and that the derivatives of the series may not converge at all. Accordingly, slow convergence of modal expansion can be expected when the applied loads exhibit discontinuities in time or space. This is demonstrated for the transient response of a string under a point load in Ref. 11, and this type of convergence problem has been referred to as a Gibbs phenomenon.<sup>12</sup> In an actively controlled structure, where most of the damping is supplied by the control system, convergence problems may be caused by point actuators.

In transient structural dynamics, methods have been developed that accelerate convergence when using mode superposition.<sup>13-16</sup> References 13-15 use a pseudostatic load (mode-acceleration method), or Ritz vectors corresponding to static displacement, to accelerate the convergence of a transient analysis. In Ref. 17, it was shown that, for a simple, direct-rate feedback control system (equivalent to some forms of passive damping), the errors in derivatives of the closed-loop eigenvalues due to modal truncation can be prohibitively large. However, it was also shown that carefully chosen Ritz vectors added to the reduced model greatly improved the accuracy of the derivatives. Similar results were shown for the eigenvalues in Ref. 18, where the Ritz vectors are called Krylov

Received July 31, 1989; revision received May 30, 1990; accepted for publication July 10, 1990. This paper is declared a work of the U.S. Government and is not subject to copyright protection in the United States.

\*Graduate Research Assistant, Department of Aerospace and Ocean Engineering; currently Senior Engineer, Martin Marietta Astronautics Group, P.O. Box 179, Mail Stop H4330, Denver, CO 80201. Member AIAA.

†Christopher Kraft Professor, Department of Aerospace and Ocean Engineering. Member AIAA.

vectors. This paper extends the work of Ref. 17 for the case of an optimal linear quadratic Gaussian (LQG) control system. In addition, this paper also examines the effect the Ritz vectors have on the design of the control system.

In the first part of the paper, we repeat the analysis of Ref. 17 for a simply supported, multispan beam with an LQG control system. The convergence of the damping ratios and their derivatives with respect to an added concentrated mass is examined. Then the procedure is repeated with the addition of Ritz vectors to the reduced model.

In the second part of the paper, we examine the effect the Ritz vectors have on the design of the control system. When a control system is designed with a reduced model, and then analyzed with the full model it is often found that the damping predicted by the reduced model is not realized in the full model. This damping shortfall is investigated for control systems designed with reduced models based on vibration modes only and for control systems designed with reduced models that include Ritz vectors.

### Analysis and Sensitivity Calculations

#### Equations of Motion

The discretized equations of motion for a flexible structure with an output-feedback control are written as

$$M\ddot{q} + D\dot{q} + Kq = U_c u \quad (1)$$

where  $M$ ,  $D$ ,  $K$ , and  $U_c$  are the mass, inherent damping, stiffness, and control influence matrices, respectively;  $q$  is the  $n$ -degree-of-freedom (DOF) displacement vector; and  $u$  is a vector of control forces. In the following derivations and examples, we will concentrate on velocity feedback; thus, we assume that  $n_v$  velocities are measured, and the sensed velocity  $y$  can be written as

$$y = U_s \dot{q} \quad (2)$$

where  $U_s$  is the sensor influence matrix.

The order of the preceding equations is typically too large for designing a control system; therefore, the order of the model is reduced by expressing the displacement vector  $q$  as a linear combination of a small number of reduced-basis vectors by

$$q = \Phi \eta \quad (3)$$

where  $\Phi$  is a matrix whose columns are reduced-basis vectors and  $\eta$  is a vector of amplitudes. In this work,  $\Phi$  may contain both natural vibration modes and Ritz vectors corresponding to static displacements; however, for this derivation, they will all be referred to as modes and the amplitudes will be referred to as modal coordinates.

Substituting Eq. (3) into Eq. (1) and premultiplying by  $\Phi^T$  gives us the equations in modal form

$$\hat{M}\ddot{\eta} + \hat{D}\dot{\eta} + \hat{K}\eta = \Phi^T U_c u \quad (4)$$

where

$$\hat{M} = \Phi^T M \Phi, \quad \hat{D} = \Phi^T D \Phi, \quad \hat{K} = \Phi^T K \Phi \quad (5)$$

Multiplying through by  $\hat{M}^{-1}$ , and writing in state form, we get

$$\begin{Bmatrix} \dot{\eta} \\ \eta \end{Bmatrix} = \begin{bmatrix} -\hat{M}^{-1}\hat{D} & -\hat{M}^{-1}\hat{K} \\ I & 0 \end{bmatrix} \begin{Bmatrix} \eta \\ \dot{\eta} \end{Bmatrix} + \begin{bmatrix} \hat{M}^{-1}\Phi^T U_c \\ 0 \end{bmatrix} u \quad (6)$$

$$\dot{x} = Ax + Bu$$

where  $x^T = [\eta^T \dot{\eta}^T]$ .

The number of modes used in the reduced model determines the accuracy of the solution. In the present work, we assume that  $n_c$  modes are used to design the control system, and then the response of the actual structure is approximated by analyzing it with additional modes. The modes with which the control system is designed are called the controlled modes and are denoted with a subscript  $c$ . The rest of the modes are called residual modes and are denoted with a subscript  $r$ . By appropriately partitioning Eq. (6), we can write the state equation in terms of controlled and residual modes as

$$\begin{Bmatrix} \dot{x}_c \\ \dot{x}_r \end{Bmatrix} = \begin{bmatrix} A_{cc} & A_{cr} \\ A_{rc} & A_{rr} \end{bmatrix} \begin{Bmatrix} x_c \\ x_r \end{Bmatrix} + \begin{bmatrix} B_c \\ B_r \end{bmatrix} u \quad (7)$$

where

$$x_c = [\eta_1 \dot{\eta}_1 \dots \eta_{n_c} \dot{\eta}_{n_c}]^T \quad (8)$$

$$x_r = [\dot{\eta}_{n_c+1} \eta_{n_c+2} \dots \dot{\eta}_r \eta_{n_c+2} \dots \eta_r]^T \quad (9)$$

Equation (2) can be transformed into modal coordinates and written in state form as

$$y = U_s \Phi \dot{\eta} = Cx = [C_c \ C_r] \begin{Bmatrix} x_c \\ x_r \end{Bmatrix} \quad (10)$$

#### Control System Design

The LQG compensator combines a linear quadratic regulator and a Kalman filter. The regulator designed on the basis of a reduced model with  $n_c$  modes produced a control output  $u$ , which minimizes the performance index

$$J = \int_0^\infty (x_c^T Q x_c + u^T R u) dt \quad (11)$$

where  $Q$  is a positive-semidefinite, state-weighting matrix and  $R$  is a positive-definite, control-weighting matrix. The unique control law that minimizes  $J$  is

$$u = -R^{-1}B_c^T P_R \hat{x}_c = -G \hat{x}_c \quad (12)$$

where  $P_R$  is a constant, symmetric, positive-semidefinite matrix that satisfies an algebraic Riccati equation, and  $\hat{x}_c$  is the current estimate of the state  $x_c$  based on the measurement  $y$ . This estimate is produced by the Kalman filter, which is defined by the equation

$$\dot{\hat{x}}_c = A_{cc} \hat{x}_c + B_c u + K_f (y - C_c \hat{x}_c) \quad (13)$$

where the filter gain matrix  $K_f$  is given by

$$K_f = P_F C_c^T V_2^{-1} \quad (14)$$

where  $P_F$  is the constant, symmetric, positive-semidefinite matrix that satisfies the algebraic Riccati equation

$$(A_{cc} + \alpha I)P_F + P_F(A_{cc} + \alpha I)^T - P_F C_c^T V_2^{-1} C_c P_F + V_1 = 0 \quad (15)$$

The matrices  $V_1$  and  $V_2$  represent the system and measurement noise, respectively. The constant  $\alpha$  is used to enforce a predetermined degree of stability to the observer poles.<sup>19</sup> By adjusting  $V_1$ ,  $V_2$ , and  $\alpha$ , the observer can be designed to satisfy a rule of thumb that requires the observer poles to be between three and ten times faster (i.e., farther left in the imaginary plane) than the regulator poles. This produces an observer that is fast enough to reconstruct the regulator state, yet slow enough not to be overly sensitive to measurement noise.

To analyze the combined regulator/observer system using residual modes, it is convenient to introduce the estimator error

$$e_c = \hat{x}_c - x_c \quad (16)$$

The full, closed-loop system with both controlled and residual modes can now be written as

$$\begin{Bmatrix} \dot{x}_c \\ \dot{e}_c \\ \dot{x}_r \end{Bmatrix} = \begin{bmatrix} A_{cc} - B_c G & -B_c G & A_{cr} \\ 0 & A_{cc} - K_f C_c & K_f C_r - A_{cr} \\ A_{rc} - B_r G & -B_r G & A_{rr} \end{bmatrix} \begin{Bmatrix} x_c \\ e_c \\ x_r \end{Bmatrix} \quad (17)$$

The closed-loop poles of Eq. (17), which are the eigenvalues of  $\bar{A}$ , can be written as

$$\lambda_k = \sigma_k + i\omega_k, \quad k = 1, 2, \dots, 4n_c + 2n_r \quad (18)$$

where  $\sigma_k$  and  $\omega_k$  are the real and imaginary parts of the eigenvalues, and  $n_c$  and  $n_r$  are the number of controlled and residual modes included in the model. The damping ratio, which is a measure of the effectiveness of the control system for a particular mode, is defined as

$$\zeta_k = \frac{-\sigma_k}{\sqrt{\sigma_k^2 + \omega_k^2}} \quad (19)$$

#### Derivative Calculation

In this study, the convergence of the control system performance ( $\zeta_k$ ) and its derivatives are to be examined. To evaluate the derivatives of the damping ratio, we need the derivatives of the closed-loop eigenvalues, which can be calculated by

$$\lambda'_k = \frac{v_k^T \bar{A}' u_k}{v_k^T u_k} \quad (20)$$

where primes denote derivatives with respect to the parameter, and where  $u_k$  and  $v_k$  are the left and right eigenvectors of the closed-loop system [Eq. (17)].

To calculate  $\bar{A}'$ , we differentiate  $A$ ,  $B$ , and  $C$  before they are split into controlled and residual modes. Once the derivatives are calculated, they can again be partitioned into the form of Eq. (17). Differentiating  $A$ , we get

$$A' = \begin{bmatrix} -(\hat{M}^{-1})' \hat{D} - \hat{M}^{-1} \hat{D}' & -(\hat{M}^{-1})' \hat{K} - \hat{M}^{-1} \hat{K}' \\ 0 & 0 \end{bmatrix} \quad (21)$$

Consider first the derivative  $(\hat{M}^{-1})'$ . Using the identity  $\hat{M}\hat{M}^{-1} = I$ , differentiating, and solving for  $(\hat{M}^{-1})'$ , we get

$$(\hat{M}^{-1})' = -\hat{M}^{-1} \hat{M}' \hat{M}^{-1} \quad (22)$$

Expanding  $\hat{M}'$ , we see that

$$\hat{M}' = \Phi^T M \Phi + \Phi^T M' \Phi + \Phi^T M \Phi' \quad (23)$$

In Ref. 17, it was found that, for the beam problem used in this study, the first and third terms can be neglected without significantly affecting the eigenvalue derivatives. This is called a fixed-mode approximation. Also, in this study, the structural parameter is an added mass so that  $K'$  and  $D'$  are zero, and with the fixed-mode approximation so are  $\hat{K}'$  and  $\hat{D}'$ .

The matrix  $M'$  is a zero matrix with a 1 on the diagonal corresponding to the location of the added mass. This now gives us all the ingredients needed to evaluate  $A'$ . Following the same procedure, we find that

$$B' = \begin{bmatrix} \hat{M}'^{-1} \Phi^T U_c \\ 0 \end{bmatrix} \quad (24)$$

and  $C' = 0$ .

Partitioning the preceding matrix derivatives, the derivative of  $\bar{A}$  with respect to an added mass can now be written as

$$\bar{A}' = \begin{bmatrix} A'_{cc} - B'_c G & -B'_c G & A'_{cr} \\ 0 & A'_{cc} & -A'_{cr} \\ A'_{rc} - B'_r G & -B'_r G & A'_{rr} \end{bmatrix} \quad (25)$$

#### Multispan Beam Example

The five-span beam shown in Fig. 1 was designed to have low-frequency, closely spaced vibration modes. The 4.5-m beam has spans of equal length, a cross-sectional area  $A = 50.0 \text{ mm}^2$ , area inertia  $I = 4.1667 \text{ mm}^4$ , weight density  $\rho = 7.6 \times 10^4 \text{ N/m}^3$ , and Young's modulus  $E = 10^9 \text{ N/m}^2$ . This results in a structure for which the first 10 frequencies are between 0.2 and 1.3 Hz. The beam is modeled with three cubic beam finite elements per span, with a total of 26 unconstrained degrees of freedom, which was shown in Ref. 17 to be quite accurate with respect to the first six natural frequencies, damping ratios, and damping ratio derivatives.

Three massless force actuators and collocated velocity sensors are placed on the beam, as shown in Fig. 1; the first and third are translation controllers on the second and fifth spans, and the second is a rotation controller on the middle span. As noted earlier, passive damping as a control device is not covered in the paper. However, the control software used for this study (ORACLS<sup>20</sup>) required the open-loop system ( $A$ ) to be stable; therefore, inherent damping is assumed to be 0.1% in each mode.

#### Convergence of Damping Ratios and Derivatives

In this study, the regulator poles are of concern; however, when looking at the closed-loop eigenvalues, it is not always possible to distinguish the regulator poles from the observer poles. Therefore, procedure was developed for keeping track of the regulator poles as the residual modes are added to the system.

Matrix  $\bar{C}$  is defined as

$$\bar{C} = \bar{A} - \beta \bar{B} \quad (26)$$

where

$$\bar{B} = \begin{bmatrix} 0 & 0 & 0 \\ 0 & 0 & K_f C_r \\ -B_r G & -B_r G & 0 \end{bmatrix} \quad (27)$$

The  $\bar{B}$  matrix contains the coupling terms between the regulator and observer; therefore, if the eigenvalues of  $\bar{C}$  are evaluated with  $\beta = 1$ , the results will always include the original regulator poles, the original observer poles, and the eigenval-

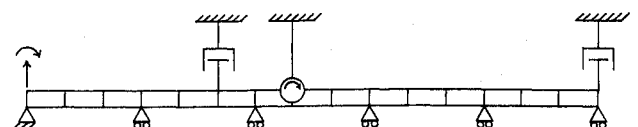


Fig. 1 Multispan beam.

Table 1 Reduced-order control design and full-model damping ratios

Mode	Regulator poles	$\zeta$	Observer poles	Full-model $\zeta$
1	(-0.16911, 1.2756)	0.13142	(-1.1045, 1.4494)	0.08653
2	(-0.11061, 1.3980)	0.07888	(-1.9939, 1.4429)	0.08077
3	(-0.23875, 1.7585)	0.13454	(-1.0311, 2.6409)	0.07801
4	(-0.13253, 2.2188)	0.05963	(-2.3056, 2.2513)	0.04618
5	(-0.33287, 2.6470)	0.12477	(-3.2626, 2.0033)	0.06935

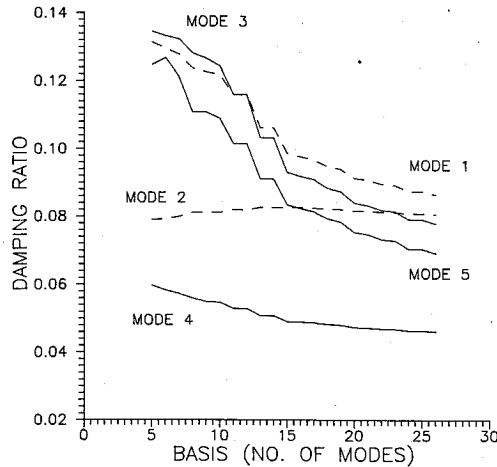


Fig. 2 Convergence of damping ratios, vibration modes only.

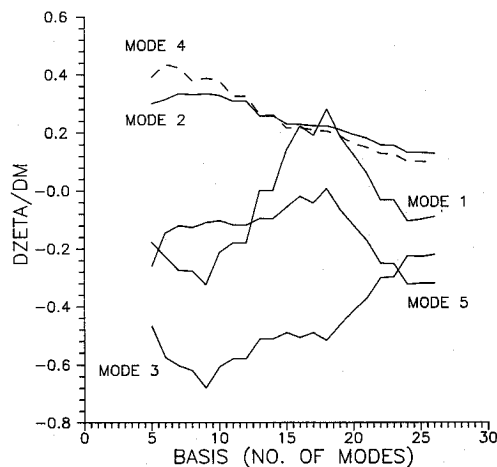


Fig. 3 Convergence of derivatives, vibration modes only.

ues corresponding to the residual modes with assumed damping of 0.1%. The regulator poles can be identified easily since they are originally well separated from the observer poles and the residual-mode eigenvalues. The values of  $\beta$  is then gradually varied from 1 to 0, and the regulator poles can be traced for a series of  $\beta$  values by using the last two regulator poles to predict the next one. The only requirement on the  $\beta$  series is that the first step is small enough so that the regulator poles do not change position with respect to the rest of eigenvalues. In this study,  $\beta_i = 1 - 2^{i-12}$  for  $i = 0, 1, \dots, 12$ .

The control system is designed based on a reduced model using the first five modes so that the damping ratios are about 0.1. This is accomplished by designing the regulator using

$$Q = \frac{1}{2} \begin{bmatrix} \Phi_c^T M \Phi_c & 0 \\ 0 & \Phi_c^T K \Phi_c \end{bmatrix} \quad (28)$$

which, when inserted in the performance index, represents the total energy in the the system, and  $R = \text{diag}(40.0, 40.0, 40.0)$ . The observer is designed so that the observer poles would satisfy the 3-to-10 rule of thumb discussed earlier. This is accomplished with a diagonal  $V_1$  with  $V_{1i} = 1$ ,  $i = 1, \dots, 4$ ,

Table 2 Percentage of error in damping ratios, vibration modes only

Basis	$\zeta_1$	$\zeta_2$	$\zeta_3$	$\zeta_4$	$\zeta_5$
5	51.84	2.333	72.47	29.06	79.93
10	40.61	0.4954	59.30	18.29	56.94
15	13.97	2.277	19.18	6.021	20.22
20	5.625	1.249	7.761	2.560	8.740
25	1.116	0.2540	1.544	0.4611	1.765

Table 3 Percentage of error in derivatives, vibration modes only

Basis	$\zeta'_1$	$\zeta'_2$	$\zeta'_3$	$\zeta'_4$	$\zeta'_5$
5	104.6	131.6	114.0	308.2	18.04
10	143.6	152.3	177.0	293.6	67.51
15	263.6	76.80	123.8	124.3	81.99
20	242.9	49.33	88.75	69.52	62.63
25	11.35	3.260	3.542	6.664	0.0214

6,  $\dots$ , 9, and  $V_{1i} = 0.1$ ,  $i = 5, 10$ ,  $V_2 = I$ , and  $\alpha = 0.50$ . Table 1 shows the regulator poles and damping ratios obtained from both the initial, five-mode reduced model and the full 26-mode model. As the table shows, the initial regulator poles vary as much as 80% from their corresponding full-model damping ratios.

#### Reduced Models with Vibration Modes Only

The damping ratios and their derivatives with respect to an added mass at the first translation controller are first calculated with the five controlled modes. The residual vibration modes are then added one at a time, and the damping ratios and derivatives are again calculated. Figures 2 and 3 show the convergence of the first five damping ratios and their derivatives vs the number of total modes used in the model. Tables 2 and 3 show the percentage of errors with respect to full-model values in the damping ratios and derivatives, respectively.

The damping ratios seem to converge fairly quickly up to about 15 modes and then slow considerably. At 15 modes, both modes 3 and 5 have errors near 20%. The convergence is slower than for the rate-feedback case in Ref. 17, where with 15 modes the damping ratios have converged to within 10%.

In Fig. 3, it is seen that the derivatives converge more slowly than the damping ratios. With a model of 15 modes, the error in derivatives of damping ratios of modes 1, 3, and 4 is still larger than 100%. With 23 out of 26 total modes, the errors in the same derivatives are larger than 30%, while the damping ratios have converged to within 10%.

The abrupt reduction in error observed in Table 3 for 25 modes is of special interest. As shown in Ref. 17, this is due to the fact that the finite-element model has 26 modes and, therefore, the error (calculated with respect to the finite element result) must go to zero for 26 modes (i.e., the finite element mode and the 26-mode model are the same). In Ref. 17, it was also shown that as the finite element model is refined, the derivatives obtained by the full finite element model do not change much, whereas the errors associated with a 25-mode model do. Thus, a 25-mode, truncated model of a higher-order, finite element model may be expected to have errors of 100 or 200% for  $\zeta'_1$  on the basis of the results for 15 and 20 modes in Table 3.

The reason for the slow convergence is that the smooth vibration modes cannot capture the discontinuities caused by the point loads. This problem is corrected by adding Ritz vectors corresponding to static displacements due to unit loads at the actuators to the reduced-basis models.

### Reduced Models with Vibration Modes and Ritz Vectors

Ritz vectors are any vectors that satisfy the geometric boundary conditions of the problem. In this study, the Ritz vectors are static displacements calculated by

$$Kq = F \quad (29)$$

where the load  $F$  is a unit load in the direction of and at the location of the actuators. Thus, in this problem, there are three Ritz vectors calculated. In Ref. 17, the Ritz vectors were normalized so that the maximum term in each vector was 1. For the LQG control system, this will not work. The Ritz vectors contain large contributions from the lower modes, thus when they are added as residual modes, the physical control is changed, as explained subsequently.

The physical control force  $u$  is given by Eq. (12), where  $G$  is a fixed gain matrix and  $\hat{x}_c$  is the current estimate of the state produced by the Kalman filter. In a physical implementation, the Kalman filter equation [Eq. (13)] would be integrated to find  $\hat{x}_c$ . If a Ritz vector is added without first making it orthogonal to the controlled modes, the modal mass matrix  $\bar{M}$  will no longer be diagonal. This will change  $A_{cc}$  via Eq. (6), which, in turn, changes the state estimation produced by the observer. Finally, this will change the physical control  $u$ . Therefore, since the control system is to remain fixed, the Ritz vectors must be made orthogonal to the controlled modes.

Letting  $v$  denote a Ritz vector, it is easy to show that a Ritz vector made orthogonal to  $n_c$  modes is given by

$$\bar{v} = v - \sum_{i=1}^{n_c} \alpha_i \phi_i \quad (30)$$

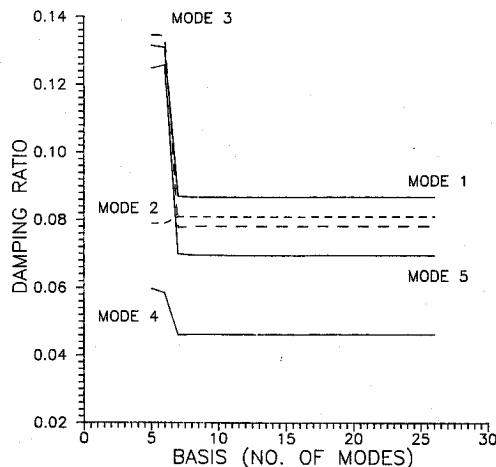


Fig. 4 Convergence of damping ratios, with Ritz vectors.

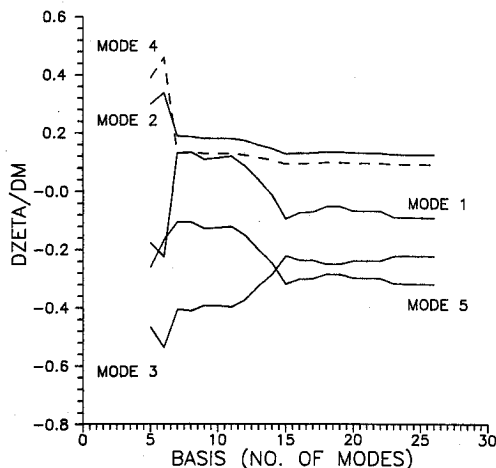


Fig. 5 Convergence of derivatives, with Ritz vectors.

where

$$\alpha_i = v^T M \phi_i \quad (31)$$

After the Ritz vectors have been made orthogonal to the controlled modes, the convergence study is repeated as before, except that the three Ritz vectors are the first to be added as residual modes. The results of the convergence studies are shown in Figs. 4 and 5. Tables 4 and 5 show the percentage of error with respect to full-model values in the damping ratios and derivatives, respectively.

Figure 4 shows a dramatic improvement in the convergence of the damping ratios. With only the five controlled modes plus three Ritz vectors, the damping ratios are essentially converged. The convergence of the derivatives with the Ritz vectors is not as good, but it is much better than in the vibration-modes-only case. The reason for the improvement in both the damping ratios and derivatives is that the higher modes are needed to model the spatial discontinuity of the actuator forces. With the Ritz vectors correctly modeling the spatial distribution of the response to actuators forces, there is no need for the higher modes.

### Ritz Vectors in Control Design

Since the Ritz vectors accelerate the convergence of the reduced model to the full model, it may be useful to include them in the reduced model used for the control system design. This section considers the possibility.

It is assumed that a small number  $n_{c1}$  of modes are to be controlled. However, to get a good design, a larger number of modes need to be included in the reduced model; that is  $n_c > n_{c1}$ . Thus the case where the additional modes are vibration modes is compared with the case where the additional modes are Ritz vectors.

Using the same structure and actuator/sensor locations,  $n_{c1} = 3$  is selected; that is a control system that controls the first three vibration modes is designed. It has already been seen from the previous example that more than three modes are needed in the control design to ensure that the damping ratios predicted by the reduced model are close to the actual damping ratios for the first three modes. The regulator and observer are designed to control the first three modes. This is accomplished with

$$Q = \frac{1}{2} \begin{bmatrix} \Phi_c^T M \Phi_c W & 0 \\ 0 & \Phi_c^T K \Phi_c W \end{bmatrix} \quad (32)$$

where  $W = \text{diag}(1.0, 1.0, 1.0, 0.01, 0.01, \dots)$ ;  $R = \text{diag}(50, 50, 50)$ ;  $V_1$  diagonal with  $V_{1i} = 1.0, i = 1, 2, 3, n_c + 1, n_c + 2, n_c + 3$  and  $V_{1ii} = 0.01$  elsewhere;  $V_2 = I$ ; and  $\alpha = 0.35$ . Designs are obtained with  $n_c$  of 5, 10, and 15 vibration modes.

For comparison, the control system is designed using three vibration modes plus three Ritz vectors, with  $W = \text{diag}(1.0,$

Table 4 Percentage of error in damping ratios, with Ritz vectors

Basis	$\zeta_1$	$\zeta_2$	$\zeta_3$	$\zeta_4$	$\zeta_5$
5	51.84	2.333	72.47	29.06	79.93
10	0.0108	0.0004	0.0299	0.0224	0.1724
15	0.0066	0.0011	0.0107	0.0066	0.0286
20	0.0034	0.0006	0.0054	0.0032	0.0131
25	0.0068	0.0014	0.0079	0.0055	0.0206

Table 5 Percentage of error in derivatives, with Ritz vectors

Basis	$\zeta'_1$	$\zeta'_2$	$\zeta'_3$	$\zeta'_4$	$\zeta'_5$
5	104.6	131.6	114.0	308.2	18.04
10	233.0	39.80	79.99	35.61	60.67
15	6.158	0.533	0.301	0.237	0.067
20	24.86	3.835	7.854	3.659	6.064
25	0.208	0.080	0.107	0.073	0.038

Table 6 Comparison of control designs: damping ratio convergence

		5	10	15	3 + 3
$\zeta_1$	Reduced model	0.120339	0.120332	0.120314	0.085201
	Full model	0.080132	0.084723	0.105898	0.085229
$\zeta_2$	Reduced model	0.071597	0.071596	0.071595	0.051270
	Full model	0.071480	0.073821	0.074609	0.051297
$\zeta_3$	Reduced model	0.127350	0.127337	0.127308	0.087033
	Full model	0.083040	0.087505	0.109849	0.087098

1.0, 1.0, 1.0, 1.0, 0.1),  $R = \text{diag}(100, 100, 100)$ ;  $V_1$  diagonal with  $V_{1ii} = 0.1$  for  $i = 6, 12$  and 1.0 elsewhere;  $V_2 = I$ ; and  $\alpha = 0.5$ .

The differences in the weighting matrices were due to the addition of the Ritz vectors in the control design. The Ritz vectors changed the reduced-order model so that if the same weighting matrices had been used, the control would not have the same performance. Thus the weighting matrices were designed so that the full-model damping ratios were between 5 and 10%.

As before, the Ritz vectors must be modified to be acceptable to the LQG control system. First, the Ritz vectors are orthogonalized with respect to the three controlled modes. Then they are made orthogonal to each other and normalized to unit mass. As before, the residual modes must be orthogonal to the controlled modes, which means that the residual modes must be made orthogonal to the modified Ritz vectors.

Table 6 shows the damping ratios predicted by a reduced-model design and compares them with damping ratios obtained with a full model for modes 1, 2, and 3. The columns labeled "5", "10", and "15" show damping ratios obtained in designs based on 5-, 10-, and 15-mode models, and the column labeled "3 + 3" shows damping ratios obtained using three vibration modes and three vectors.

The rows labeled "Reduced model" show damping ratios obtained by including only the modes used in the control design, and the rows labeled "Full model" show damping ratios obtained with all of the residual modes added.

Table 6 shows that reduced-model designs based on vibration modes only suffer from loss of performance due to model truncation. For example, for the first mode, we attempt to design 12% damping, but with five vibration modes in the reduced-model control design, the control system actually provides only 8% damping. As more modes are added to the reduced-model design, the difference becomes smaller, but even with a 15-mode model we get only 10.6% actual damping. When the Ritz vectors are added to the reduced-model design, the reduced and full-model damping ratios are nearly identical.

### Conclusions

This paper has investigated the errors in closed-loop damping ratios due to the use of reduced models based on vibration modes in the analysis and design of active vibration-control systems. It was shown for a simply supported multispan beam that both the damping ratios and derivatives with respect to an added mass converge slowly with an increasing number of modes, but with the derivatives converging much slower than the damping ratios. However, if Ritz vectors corresponding to static displacements due to unit loads at the actuators were added to the reduced model, the convergence of both the damping ratios and derivatives were greatly accelerated. It was also shown that the addition of Ritz vectors in the reduced-model control design greatly improved the agreement between the design damping ratios and the actual damping ratios. Thus, it appears that these Ritz vectors added to the reduced

models of flexible structures greatly improved the accuracy of both the analysis and design of the structure with an active control system.

### Acknowledgment

This research was supported by NASA Grant NAG-1-603.

### References

- <sup>1</sup>Rao, S. S., Venkayya, V. B., and Khot, N. S., "Game Theory Approach for the Integrated Design of Structures and Controls," *AIAA Journal*, Vol. 26, No. 4, 1988, pp. 463-469.
- <sup>2</sup>Lim, K. B., and Junkins, J. L., "Robust Optimization of Structural and Controller Parameters," *Journal of Guidance, Control, and Dynamics*, Vol. 12, No. 1, 1989, pp. 89-96.
- <sup>3</sup>Hale, A. L., Lisowski, R. J., and Dahl, W. E., "Optimal Simultaneous Structural and Control Design of Maneuvering Flexible Spacecraft," *Journal of Guidance, Control, and Dynamics*, Vol. 8, No. 1, 1985, pp. 86-93.
- <sup>4</sup>Onoda, J., and Haftka, R. T., "An Approach to Structure/Control Optimization for Large Space Structures," *AIAA Journal*, Vol. 25, No. 8, 1987, pp. 1133-1138.
- <sup>5</sup>Balas, M. J., "Active Control of Flexible Systems," *Journal of Optimization Theory and Applications*, Vol. 25, No. 3, July 1978, pp. 415-436.
- <sup>6</sup>Czajkowski, E., and Preumont, A., "Spillover Stabilization and Decentralized Modal Control of Large Space Structures," *Proceedings of the AIAA/ASME/ASCE/AHS 28th Structures, Structural Dynamics and Materials Conference*, Pt. 2B, AIAA, New York, 1987, pp. 599-609.
- <sup>7</sup>Hughes, P. C., "Space Structure Vibration Modes: How Many Exist? Which Ones Are Important?" *IEEE Control Systems Magazine*, Vol. 7, No. 1, 1987, pp. 22-28.
- <sup>8</sup>Skelton, R. E., Hughes, P. C., and Hablani, H. B., "Order Reduction for Models of Space Structures Using Modal Cost Analysis," *Journal of Guidance, Control, and Dynamics*, Vol. 5, No. 4, 1982, pp. 351-357.
- <sup>9</sup>Perry, C. O., and Venkayya, V. B., "Issues of Order Reduction in Active Control System Design," *AIAA Paper 86-2138*, Aug. 1986.
- <sup>10</sup>Haftka, R. T., and Yates, E. C., Jr., "Repetitive Flutter Calculations in Structural Design," *Journal of Aircraft*, Vol. 13, No. 7, 1976, pp. 454-461.
- <sup>11</sup>Haftka, R. T., and Kamat, M. P., *Elements of Structural Optimization*, Martinus Nijhoff, The Netherlands, 1985, pp. 172-173.
- <sup>12</sup>Tadikonda, S. S. K., and Baruh, H., "Gibbs Phenomenon in Structural Mechanics," *Proceedings of AIAA/ASME/ASCE/AHS/ASC 30th Structures, Structural Dynamics and Materials Conference*, Pt. 1, AIAA, Washington, DC, April 1989, pp. 337-347.
- <sup>13</sup>Yiu, Y. C., "Selective Modal Extraction for Dynamic Analysis of Space Structures," *Proceedings of AIAA/ASME/ASCE/AHS/ASC 30th Structures, Structural Dynamics and Materials Conference*, AIAA, Washington, DC, Pt. 1, April 1989, pp. 21-31.
- <sup>14</sup>Kline, K. A., "Dynamic Analysis Using a Reduced Basis of Exact Modes and Ritz Vectors," *AIAA Journal*, Vol. 24, No. 12, 1986, pp. 2022-2029.
- <sup>15</sup>Cornwell, R. E., Craig, R. R., Jr., and Johnson, C. P., "On the Application of the Mode-Acceleration Method to Structural Engineering Problems," *Earthquake Engineering and Structural Dynamics*, Vol. 11, No. 5, 1983, pp. 679-688.
- <sup>16</sup>Carmada, C. J., and Haftka, R. T., "Development of Higher-Order Modal Methods for Transient Thermal and Structural Analysis," NASA TM-101548, Feb. 1989.
- <sup>17</sup>Sandridge, C. A., and Haftka, R. T., "Accuracy of Eigenvalue Derivatives from Reduced Order Structural Models," *Journal of Guidance, Control, and Dynamics*, Vol. 12, No. 6, 1989, pp. 822-829.
- <sup>18</sup>Su, T.-J., and Craig, R. R., Jr., "Model Reduction and Control of Flexible Structures Using Krylov Subspaces," *Proceedings of the AIAA/ASME/ASCE/AHS 30th Structures, Structural Dynamics and Materials Conference*, Pt. 2, AIAA, Washington, DC, 1989, pp. 691-700.
- <sup>19</sup>Anderson, B. D. O., and Moore, J. B., *Linear Optimal Control*, Prentice-Hall, Englewood Cliffs, NJ, 1971, pp. 50-60.
- <sup>20</sup>Armstrong, E. S., *ORACLS: A Design System for Linear Multivariate Control*, Marcel Dekker, New York, 1980.